

Thermal, Squeezing and Compressibility Effects in Lubrication of Asymmetric Rollers

D. Prasad^a, S.V. Subrahmanyam^b, S.S. Panda^c

^aDr. S.R.K. Govt. Arts College, Yanam, India,

^bK.L. University, Guntur, India,

^cRegency Institute of Technology, Yanam, India.

Keywords:

*Hydrodynamic lubrication
Non-Newtonian
Power law
Thermal effects
Squeezing
Compressibility
Consistency*

ABSTRACT

Hydrodynamically heavily loaded rigid cylindrical rollers, lubricated by a thin compressible fluid film, are investigated for normal squeezing motion and cavitations. The lubricant is assumed to follow the non-Newtonian power-law fluid model where consistency and density of the lubricant vary with one dimensional pressure and temperature. The modified Reynolds pressure equation and thermal energy equation are derived and solved simultaneously by R-K Fehlberg method. Secant method is also applied in order to enforce the boundary condition at the outlet. It is observed that temperature has significant effects on consistency and density both. It is also to be noted that compressibility effect is even more significant when squeezing is taken into account.

Corresponding author:

*S.V. Subrahmanyam,
K.L. University, Guntur-522502, Andhra
Pradesh, India
E-mail: subrahmanyam@kluniversity.in*

© 2014 Published by Faculty of Engineering

1. INTRODUCTION

A contact between two surfaces is of great importance in technology. At the interface of two materials, when they brought together, separated or moved with respect to one another, contact information, friction, wear and lubrication are the processes that occur [1].

Further, the Squeeze films play an important role in the analysis of the dynamic behavior of bearings and, in general, many practical engineering systems. In order to model such system proper knowledge of the forces generated by the squeeze film in between solid

boundaries is necessary [2]. This situation occurs frequently in many machine components such as gear teeth, cams, automotive engines, aircraft engines, rolling elements, machine tools, skeletal joints, the bearings in reciprocating engines and many more [3]. In this regard, Dowson et al. [4] initiated the comprehensive study of squeezing motion of Newtonian lubrication of cylindrical rollers and obtained the solution for a wide range of parameters. Sinha et al. [5] examined this problem with squeezing motion for non-Newtonian power law lubricant. Prasad et al [6] extended the same result with cavitation while adding thermal effect where the consistency of the lubricant was

assumed to vary with pressure and the mean temperature. Later, Rong-Tsonn and Hamrock [7] made a comprehensive study of isothermal Newtonian lubrication of both rigid and EHD line contacts with compressibility and squeezing. Usha and Rukmani Sridharan [2] investigated the laminar squeeze flow of an incompressible Newtonian fluid between non-rotating annular surfaces including all inertial terms in the governing equations of motion and a solution has been obtained in terms of a single non-dimensional squeeze Reynolds number S , for small values of S . J-R Lin et al. [8] derived a general dynamic Reynolds equation of sliding squeezing surfaces with non-Newtonian fluids for the assessment of dynamic characteristics of a lubricating system and the transient squeezing action effect is taken into account while considering the effect of couple stresses resulting from the lubricant blended with various additives. Jaffar [3] studied a line contact problem with squeezing effect, and various results were reported for a wide range of layer thickness, the layer compressibility and the central squeeze film velocity. Bujurke et al. [9] observed the effects of surface roughness on the characteristics of squeeze film lubrication between curved annular plates, and it was found that the effect of radial (circumferential) roughness pattern is to shift the point of maximum pressure towards the inlet (outlet) edge. Further, it was observed that the mean load carrying capacity was found to increase (decrease) for the circumferential (radial) roughness pattern compared with the corresponding smooth case for both concave and convex pad geometries. Naduvinamani et al [10] made some investigations to study the combined effects of unidirectional surface roughness and magnetic effect on the performance characteristics of porous squeeze film lubrication between two rectangular plates and it was observed that a roughness effect enhances pressure, load carrying capacity and squeeze film time. Recently, Li-Ming Chu et al [11] developed a numerical method for general applications with effects of surface force to investigate the pure squeezing action within an isothermal thin film EHL spherical conjunction under constant load condition. Later, Jaw-Ren Lin [12] presented a theoretical study of the non-Newtonian effects on the squeeze film characteristics between parallel annular disks on the basis of Rabinowitsch fluid model. A closed form solution was derived using a small perturbation method.

One of the other realistic conditions, which play an important role in lubrication theory, is compressibility effect. In fact, the compressibility of liquid fluids under typical engineering conditions is not normally an issue, and most fluid mechanics analyses can be performed assuming liquid incompressibility. However, in concentrated lubricated contacts, such as those formed in rolling element bearings, gears, cams, and constant velocity joints, etc., it is not uncommon for the lubricants to be subjected to pressure variations within the contact regions of around 10^9 pa and higher. Under these conditions significant reductions in fluid volume can be experienced [13].

Generally it may be difficult to consider liquids as compressible media, but in high loaded EHL contacts, the compressibility variation of the lubricant is certainly not negligible. At high loads, the compression of the lubricant has a significant influence on the film thickness variation inside the contact. A number of different density models have been used in EHL calculations through the year [14]. Prasad et al [15] considered a problem of heavily loaded rigid cylindrical rollers, lubricated by a thin compressible power-law fluid assuming the consistency and density of the lubricant vary with temperature and pressure. As a result, it was observed that for low values of power-law index n there was no significant effect to pressure and temperature on the consistency. Even the compressibility effects are not very significant for those low values. Hsiao-Ming Chu et al [16] derived a one dimensional modified Reynolds equation with power-law fluid from the viscous adsorption theory for thin film EHL including pressure- viscosity, pressure- density characteristics of the lubricant and the visco-elastic deformation of the rollers. Finally, the film shape and the pressure distribution under pure rolling conditions are numerically calculated and discussed for various operating conditions. Moraru and Keith [17] presented a Lobatto point quadrature algorithm which is applicable for TEHL problem where both density and viscosity of the lubricant are taken to be temperature and pressure dependent, and the transverse velocity term in the energy equation is obtained from the continuity equation. Use of the Lobatto point calculation method has resulted in accuracy without the use of a larger number of grid points. Mircea D. Pascovici et al.

[18] proposed a model for the squeeze process under impact for highly compressible porous layers imbibed with fluids. It was assumed that the normal forces generated by the elastic compression of the fibers comprising the solid face are negligible compared to the pressure forces generated in the imbibed fluid, within the porous layer. It was demonstrated for the rectangular plates that the square plates could minimize the maximum squeeze induced load. Stolarski [19] verified the transient film pressure of a squeeze film gas bearing experimentally with comparison to numerical results obtained from the Reynolds equation. These two results were in good agreement with CFD result for small vibrating amplitudes. Bayada and Chupin [20] had shown how vaporous cavitation in lubricant films can be modeled in a physically justified manner through the constitutive (compressibility) relation of the fluid. It is found that how the widely used Jakobsson–Floberg–Olsson (JFO) / Elrod–Adams (EA) mass flow conservation model can be compared with this new model. Moreover, the new model can incorporate the variation of the viscosity in the cavitation region and allows the pressure to fall below a cavitation pressure and numerical computations show that discrepancy with JFO/EA is mostly associated with light loading condition, starved situation or viscosity effects. Habchi and Bair [21] investigated the effects of lubricant compressibility on the film-forming performance of thermal elastohydrodynamic lubricated (EHL) circular contacts. Numerical film thickness predictions using the classical Dowson and Higginson relationship are compared to those that would be obtained using a more realistic compressibility model. As a result it is highlighted that highlights the importance of using realistic transport properties modeling based on thermodynamic scaling for an accurate numerical prediction of the performance of EHL contacts. Nadim A. Diab and Issam Lakkis [22] investigated the effect of various assumptions proposed by the classical Reynolds lubrication equation. In particular, a microplate oscillating at high frequencies (beyond cutoff) and high velocities leading to appreciable displacement within the film gap is studied. Andreas Almqvist et al. [23] proposed a theory based on clear physical arguments related to conservation of mass flow and considers both incompressible and compressible

fluids. The result of the mathematical modeling is a system of equations with two unknowns, which are related to the hydrodynamic pressure and the degree of saturation of the fluid. The model and the associated numerical solution method have significant advantages over today's most frequently used cavitation algorithms, which are based on Elrod–Adams pioneering work.

In addition, it is well known that the pressure, the temperature and the film shape definitely play an important role in the failure of heavily loaded non-conformal contacts. In fact, the effect of heat generated due to the shearing of the high pressure lubricant is no longer negligible under sliding conditions, as the heat changes the characteristics of the oil flow because of a decrease in viscosity. Therefore, thermal effect on the film thickness and traction is significant in EHL contacts [24]. Further, temperature rise in lubricant film occurs due to rapid shear of lubricant layers. The hydrodynamic action is affected due to the thermal effects [25].

Non-Newtonian behavior of the lubricants has also been addressed severely. Because the lubricants used in every day machines are seldom single component liquids. In fact some base oil is mixed with them. The base oils are often blends of different molecular weight “cuts” to arrive at a special ambient pressure viscosity. Also, viscosity modifying polymer additives are often blended with the base oil. In particular, the lubricants used in automobiles are usually mixtures. The non-Newtonian behavior of solutions of high-molecular-weight polymers in low-molecular-weight solvents, in shear flow and in extensional flow, has been subject of much attention in rheology [26,27]. The temperature rise for a non-Newtonian lubricant can be better estimated using power law lubricant [25].

The very purpose of lubrication is to separate surfaces to relative motion in order to reduce friction and wear. The separation and load carrying capacity are achieved by generating a pressure in the fluid film between the surfaces. The most significant pressure build-up in hydrodynamic lubrication is achieved when a converging gap is allowed to form the surfaces. In order to improve performance and efficiency, and to reduce wear and risk of failure in hydrodynamic lubrication, it is important to study various effects that can contribute to the pressure build-up [28].

Hence, in order to incorporate those various effects of surface forces on squeeze thin film non-Newtonian lubrication of rolling/sliding line contact problem including compressibility and cavitations, the modified Reynolds equation, the energy equation and the lubricant rheology equation are solved simultaneously. Also for semi analytical solution, the surfaces are assumed to be smooth and rigid. The consistency and the density of the lubricant are assumed to vary with pressure and temperature. An efficient method of numerical solution with good accuracy is employed to solve the above equations.

2. THEORETICAL MODEL

2.1 Momentum and Continuity Equations

For, the parallel cylinders [29] the basic flow momentum and continuity equations for a compressible power law fluid under consideration may be written as follows [15]:

$$\frac{dp}{dx} = \frac{\partial}{\partial y} \left(m \left| \frac{\partial u}{\partial y} \right|^{n-1} \frac{\partial u}{\partial y} \right) \quad (1)$$

$$\frac{\partial}{\partial x}(\rho u) + \frac{\partial}{\partial y}(\rho v) = 0 \quad (2)$$

where the consistency 'm' and density 'ρ' of the lubricant are assumed to vary with pressure and temperature as per the following relationships [30,31]:

$$m = m_0 e^{\alpha p - \beta (T - T_0)} \quad (3)$$

$$\rho = \rho_0 \left[1 + \frac{c_1 p}{1 + c_2 p} - D_T (T - T_0) \right] \quad (4)$$

where c_1 and c_2 are density-pressure coefficients, D_T is density-temperature coefficient.

2.2 Boundary Conditions

$$\left. \begin{aligned} u=U_1 \text{ and } v &= \frac{-V}{2} - U_1 \frac{dh}{dx} \text{ at } y=-h \\ u=U_2 \text{ and } v &= \frac{V}{2} + U_2 \frac{dh}{dx} \text{ at } y=h \end{aligned} \right\} \quad (5)$$

$$p=0 \text{ at } x=-\infty, \text{ and } p=\frac{dp}{dx}=0 \text{ at } x=x_2 \quad (6)$$

$$\text{where } h = h_0 + \frac{x^2}{2R} \quad (7)$$

where U_1 and U_2 are velocities of the rolling cylinders as shown in Fig. (1).

From the geometry, one may observe that for each x, $\frac{\partial u}{\partial y} = 0$ at $y = \delta$ ($-h \leq \delta \leq h$) in both

the regions: I: $-\infty < x \leq -x_1$ and

II: $-x_1 \leq x \leq x_2$.

Further, these two regions may be divided into four sub regions separated by δ profile having velocities u_1, u_2, u_3 and u_4 . Assuming the velocity gradients for the geometry under consideration, those may be written as:

$$\left. \begin{aligned} \frac{\partial u_1}{\partial y} &\geq 0, \delta \leq y \leq h \\ \frac{\partial u_2}{\partial y} &\leq 0, -h \leq y \leq \delta \end{aligned} \right\} \text{I: } -\infty < x \leq -x_1 \quad (8)$$

$$\left. \begin{aligned} \frac{\partial u_3}{\partial y} &\geq 0, -h \leq y \leq \delta \\ \frac{\partial u_4}{\partial y} &\leq 0, \delta \leq y \leq h \end{aligned} \right\} \text{II: } -x_1 \leq x \leq x_2 \quad (9)$$

Using the sign of the velocity gradients mentioned in (8) and the pressure gradient, integration of equation (1) twice for the region: $-\infty < x \leq -x_1$; one may obtain:

$$u_1 = U_2 + \left(\frac{n}{n+1} \right) \left(\frac{1}{m_1} \frac{dp_1}{dx} \right)^{\frac{1}{n}} \left[(y-\delta)^{\frac{n+1}{n}} - (h-\delta)^{\frac{n+1}{n}} \right], \quad \delta \leq y \leq h \quad (10)$$

$$u_2 = U_1 + \left(\frac{n}{n+1} \right) \left(\frac{1}{m_1} \frac{dp_1}{dx} \right)^{\frac{1}{n}} \left[(\delta-y)^{\frac{n+1}{n}} - (\delta+h)^{\frac{n+1}{n}} \right], \quad -h \leq y \leq \delta \quad (11)$$

In the same way, for the region, $-x_1 \leq x \leq x_2$:

$$u_3 = U_1 + \left(\frac{n}{n+1} \right) \left(\frac{1}{m_2} \frac{dp_2}{dx} \right)^{\frac{1}{n}} \left[(\delta+h)^{\frac{n+1}{n}} - (\delta-y)^{\frac{n+1}{n}} \right], \quad -h \leq y \leq \delta \quad (12)$$

$$u_4 = U_2 + \left(\frac{n}{n+1} \right) \left(\frac{1}{m_2} \frac{dp_2}{dx} \right)^{\frac{1}{n}} \left[(h-\delta)^{\frac{n+1}{n}} - (y-\delta)^{\frac{n+1}{n}} \right], \quad \delta \leq y \leq h \quad (13)$$

Now, solving the continuity equation (2) using (5), one may get:

$$\rho V + \frac{d}{dx} \left\{ \rho \left[h(U_1+U_2) + \delta(U_1-U_2) - \left(\frac{n}{2n+1} \right) \left(\frac{1}{m_1} \frac{dp_1}{dx} \right)^{\frac{1}{n}} \left[(h+\delta)^{\frac{2n+1}{n}} + (h-\delta)^{\frac{2n+1}{n}} \right] \right] \right\} = 0, \quad -\infty < x \leq -x_1 \quad (14)$$

$$\rho_2 V + \frac{d}{dx} \left\{ \rho_2 \left[h(U_1 + U_2) + \delta(U_1 - U_2) + \left(\frac{n}{2n+1} \right) \left(\frac{-1}{m_2} \frac{dp_2}{dx} \right)^{\frac{1}{n}} \left[(h+\delta)^{\frac{2n+1}{n}} + (h-\delta)^{\frac{2n+1}{n}} \right] \right] \right\} = 0 \quad (15)$$

$$, -x_1 \leq x \leq x_2$$

Let

$$-r_1 = \rho_1 \left[h(U_1 + U_2) + \delta(U_1 - U_2) - \left(\frac{n}{2n+1} \right) \left(\frac{1}{m_1} \frac{dp_1}{dx} \right)^{\frac{1}{n}} \left[(h+\delta)^{\frac{2n+1}{n}} + (h-\delta)^{\frac{2n+1}{n}} \right] \right] \quad (16)$$

and

$$-r_2 = \rho_2 \left[h(U_1 + U_2) + \delta(U_1 - U_2) + \left(\frac{n}{2n+1} \right) \left(\frac{-1}{m_2} \frac{dp_2}{dx} \right)^{\frac{1}{n}} \left[(h+\delta)^{\frac{2n+1}{n}} + (h-\delta)^{\frac{2n+1}{n}} \right] \right] \quad (17)$$

so that the equations (14) and (15) reduce to:

$$\frac{dr_1}{dx} = \rho_1 V \quad (18)$$

$$\frac{dr_2}{dx} = \rho_2 V \quad (19)$$

2.3 Reynolds equation

From equations (16) and (17), one may obtain:

$$\frac{dp_1}{dx} = m_1 \left(\frac{2n+1}{n} \right)^n \left[\frac{r_1 + \rho_1 [(U_1 + U_2)h + (U_1 - U_2)\delta]}{\rho_1 [(h+\delta)^{\frac{2n+1}{n}} + (h-\delta)^{\frac{2n+1}{n}}]} \right], \quad (20)$$

$$-\infty < x \leq -x_1$$

$$\frac{dp_2}{dx} = -m_2 \left(\frac{2n+1}{n} \right)^n \left[\frac{-r_2 - \rho_2 [(U_1 + U_2)h + (U_1 - U_2)\delta]}{\rho_2 [(h+\delta)^{\frac{2n+1}{n}} + (h-\delta)^{\frac{2n+1}{n}}]} \right], \quad (21)$$

$$-x_1 \leq x \leq x_2$$

Using the velocity matching conditions:

$u_1 = u_2$ and $u_3 = u_4$ at $y = \delta$ one can get:

$$(U_1 - U_2) + \left(\frac{n}{n+1} \right) \left(\frac{1}{m_1} \frac{dp_1}{dx} \right)^{\frac{1}{n}} \left[(h-\delta)^{\frac{n+1}{n}} - (h+\delta)^{\frac{n+1}{n}} \right] = 0, \quad (22)$$

$$-\infty < x \leq -x_1$$

$$(U_1 - U_2) - \left(\frac{n}{n+1} \right) \left(\frac{-1}{m_2} \frac{dp_2}{dx} \right)^{\frac{1}{n}} \left[(h-\delta)^{\frac{n+1}{n}} - (h+\delta)^{\frac{n+1}{n}} \right] = 0, \quad (23)$$

$$-x_1 \leq x \leq x_2$$

Eliminating $\frac{dp_1}{dx}$ and $\frac{dp_2}{dx}$ from equation (22) and (23) and using Reynolds equation (20) and (21), one can obtain:

$$(U_2 - U_1) + \left(\frac{2n+1}{n+1} \right) \left[\frac{r_1 + \rho_1 [(U_1 + U_2)h + (U_1 - U_2)\delta]}{\rho_1 [(h+\delta)^{\frac{2n+1}{n}} + (h-\delta)^{\frac{2n+1}{n}}]} \right] \left[(h+\delta)^{\frac{n+1}{n}} - (h-\delta)^{\frac{n+1}{n}} \right] = 0 \quad (24)$$

$$, -\infty < x \leq -x_1$$

$$(U_2 - U_1) + \left(\frac{2n+1}{n+1} \right) \left[\frac{r_2 + \rho_2 [(U_1 + U_2)h + (U_1 - U_2)\delta]}{\rho_2 [(h+\delta)^{\frac{2n+1}{n}} + (h-\delta)^{\frac{2n+1}{n}}]} \right] \left[(h+\delta)^{\frac{n+1}{n}} - (h-\delta)^{\frac{n+1}{n}} \right] = 0 \quad (25)$$

$$, -x_1 \leq x \leq x_2$$

2.4 Energy Equation

The governing equation for the temperature distribution of the lubricant for the power-law fluid including compressibility may be written as [32]:

$$\rho c_p u \frac{\partial T}{\partial x} = K \frac{\partial^2 T}{\partial y^2} + m \left| \frac{\partial u}{\partial y} \right|^{n-1} \left(\frac{\partial u}{\partial y} \right)^2 + \epsilon T u \frac{dp}{dx} \quad (26)$$

where the last term of (26) is the heat of compression [30]. The heat of convection is dominant in the inlet region and when the bearing is running at high speed; its dominance is extended towards its central zone as well. On the other hand, the heat of conduction is dominant in the central zone and if the boundaries are assumed to be adiabatic the heat does not go out of the boundaries through conduction. So, the heat lost by conduction is less and may be dropped [32-34]. Since the heat does not go out of the adiabatic boundaries (in Y-direction), it is carried away by the lubricant itself, the temperature of the lubricant may be assumed to be one dimensional that is a function of x only [15]. Hence equation (26) is reduced to:

$$\rho c_p u \frac{dT}{dx} = m \left| \frac{\partial u}{\partial y} \right|^{n-1} \left(\frac{\partial u}{\partial y} \right)^2 + \epsilon T u \frac{dp}{dx} \quad (27)$$

where c_p is the specific heat of the lubricant at constant pressure. Using the following temperature boundary condition:

$$T = T_0 \text{ at } x = -\infty \quad (28)$$

the film temperature can be obtained by integrating equation (27) with respect to y over the film thickness and using conditions (5), one may obtain as follows:

$$\frac{dT_1}{dx} = m_1 \left(\frac{2n+1}{n} \right)^n \left[\frac{r_1 + \rho_1 [(U_1 + U_2)h + (U_1 - U_2)\delta]}{\rho_1 [(h+\delta)^{\frac{2n+1}{n}} + (h-\delta)^{\frac{2n+1}{n}}]} \right] \left[\frac{r(\epsilon T - 1) - \rho_1 [(U_1 + U_2)h + (U_1 - U_2)\delta]}{r \rho c_p} \right], \quad (29)$$

$$-\infty < x \leq -x_1$$

$$\frac{dT_2}{dx} = -m_2 \left(\frac{2n+1}{n} \right)^n \left[\frac{-r_2 - \rho_2 [(U_1+U_2)h + (U_1-U_2)\delta]}{\rho_2 \left[(h+\delta)^{\frac{2n+1}{n}} + (h-\delta)^{\frac{2n+1}{n}} \right]} \right] \left[\frac{s(\varepsilon T_1 - 1) - \rho_2 [(U_1+U_2)h + (U_1-U_2)\delta]}{s\rho_2 C_p} \right]$$

$$-x_1 \leq x \leq x_2 \quad (30)$$

Now, using the following dimensionless scheme:

$$\bar{x} = \frac{x}{\sqrt{2Rh_0}}, \bar{m} = 2m_0 c_1, \bar{p} = c_1 p, c_n = \frac{1}{2} \left(\frac{2n+1}{n} \right)^n \left(\frac{U}{h_0} \right)^n \sqrt{\frac{2R}{h_0}},$$

$$\bar{h} = 1 + \bar{x}^2, \bar{T}_m = \beta T_m, \bar{\delta} = \delta/h_0, \bar{U} = U_2/U_1, \bar{h} = h/h_0,$$

$$\bar{V} = \frac{V}{U_1 \sqrt{\frac{2R}{h_0}}}, \bar{\rho} = \rho/\rho_0, \bar{\varepsilon} = \varepsilon/\beta, \bar{r} = \frac{r}{\rho_0 U_1 h_0}, \text{ etc.}$$

The above equations (18), (19), (20), (21), (24), (28) and (29) can be written as

$$\frac{d\bar{r}}{d\bar{x}} = \bar{\rho}_1 \bar{V} \quad (32)$$

$$\frac{d\bar{s}}{d\bar{x}} = \bar{\rho}_2 \bar{V} \quad (33)$$

$$\frac{d\bar{p}_1}{d\bar{x}} = \bar{m}_1 (\bar{f})^n \quad (34)$$

$$\frac{d\bar{p}_2}{d\bar{x}} = -\bar{m}_2 (-\bar{g})^n \quad (35)$$

$$(\bar{U}-1) + \left(\frac{2n+1}{n+1} \right) \left[(\bar{h}+\bar{\delta})^{\frac{n+1}{n}} - (\bar{h}-\bar{\delta})^{\frac{n+1}{n}} \right] (\bar{f}) = 0 \quad (36)$$

$$(\bar{U}-1) + \left(\frac{2n+1}{n+1} \right) \left[(\bar{h}+\bar{\delta})^{\frac{n+1}{n}} - (\bar{h}-\bar{\delta})^{\frac{n+1}{n}} \right] (\bar{g}) = 0 \quad (37)$$

$$\frac{d\bar{T}_1}{d\bar{x}} = \bar{m}_1 \bar{\gamma} (\bar{f})^n \bar{\psi}_1 \quad (38)$$

$$\frac{d\bar{T}_2}{d\bar{x}} = -\bar{m}_2 \bar{\gamma} (-\bar{g})^n \bar{\psi}_2 \quad (39)$$

Where

$$\bar{\rho} = 1 + \frac{\bar{p}}{1 + A\bar{p}} - \bar{D}_T (\bar{T} + \bar{T}_0) \quad (40)$$

$$\bar{m}_1 = \bar{m}_0 e^{(B\bar{p}_1 - \bar{T} + \bar{T}_0)}, \text{ etc.} \quad (41)$$

Where $A = c_2/c_1$, and $B = \alpha/c_1$

$$\bar{f} = \frac{\bar{r}_1 + \bar{\rho}_1 \left[(\bar{U}+1)\bar{h} + (1-\bar{U})\bar{\delta} \right]}{\bar{\rho}_1 \left[(\bar{h}+\bar{\delta})^{\frac{2n+1}{n}} + (\bar{h}-\bar{\delta})^{\frac{2n+1}{n}} \right]} \quad (42)$$

$$\bar{g} = \frac{\bar{r}_2 + \bar{\rho}_2 \left[(\bar{U}+1)\bar{h} + (1-\bar{U})\bar{\delta} \right]}{\bar{\rho}_2 \left[(\bar{h}+\bar{\delta})^{\frac{2n+1}{n}} + (\bar{h}-\bar{\delta})^{\frac{2n+1}{n}} \right]} \quad (43)$$

$$\bar{\gamma} = \left(\frac{\beta}{\rho_0 c_1 c_p} \right) \quad (44)$$

$$\bar{\psi}_1 = \frac{\bar{r}_1 (\varepsilon \bar{T}_1 - 1) - \bar{\rho}_1 \left[(\bar{U}+1)\bar{h} + (1-\bar{U})\bar{\delta} \right]}{\bar{r}_1 \bar{\rho}_1} \quad (45)$$

$$\bar{\psi}_2 = \frac{\bar{r}_2 (\varepsilon \bar{T}_2 - 1) - \bar{\rho}_2 \left[(\bar{U}+1)\bar{h} + (1-\bar{U})\bar{\delta} \right]}{\bar{r}_2 \bar{\rho}_2} \quad (46)$$

2.5 Load and Traction

The load components W in the y-direction is calculated as:

$$W = \int_{-\infty}^{x_2} p \, dx \quad (47)$$

The dimensionless load $\bar{W} = \frac{w\alpha}{\sqrt{2Rh_0}}$ is given by:

$$\bar{W} = \int_{-\infty}^{\bar{x}_2} \bar{p} \, d\bar{x} = - \int_{-\infty}^{\bar{x}_2} \bar{x} \frac{d\bar{p}}{d\bar{x}} \, d\bar{x} \quad (48)$$

The surface traction force is obtained from the integration of shear stress τ over the entire fluid flow regions; and one may get:

$$T_{Fh-} = - \int_{-\infty}^{x_2} \tau_{y=-h} \, dx \quad (49)$$

$$T_{Fh+} = - \int_{-\infty}^{x_2} \tau_{y=h} \, dx \quad (50)$$

Dimensionless tractions are:

$$\bar{T}_{Fh-} \left(= \alpha \frac{T_{F0}}{h_0} \right) = - \int_{-\infty}^{\bar{x}_2} \bar{\tau}_{y=-\bar{h}} \, d\bar{x} \quad (51)$$

$$\bar{T}_{Fh+} = - \int_{-\infty}^{\bar{x}_2} \bar{\tau}_{y=\bar{h}} \, d\bar{x} \quad (52)$$

3. RESULTS AND DISCUSSION

A typical semi analytical solution of the modified Reynolds equations (34), (35) and the energy equations (38), (39) have been obtained for symmetrical and asymmetrical, viscous compressible flow of power law fluids throughout the gap between two cylinders, Fig. 1. The results of the investigation are assessed in terms of parameters n , \bar{U} ($=U_2/U_1$, $U_2 > U_1$) and \bar{V} .

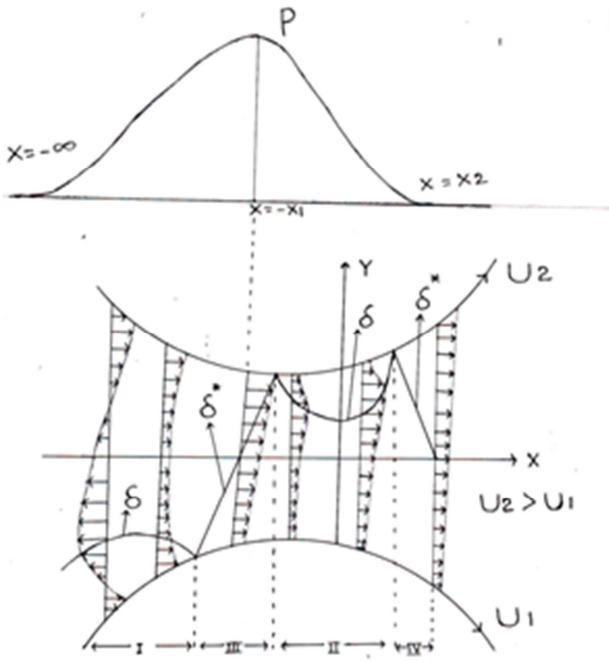


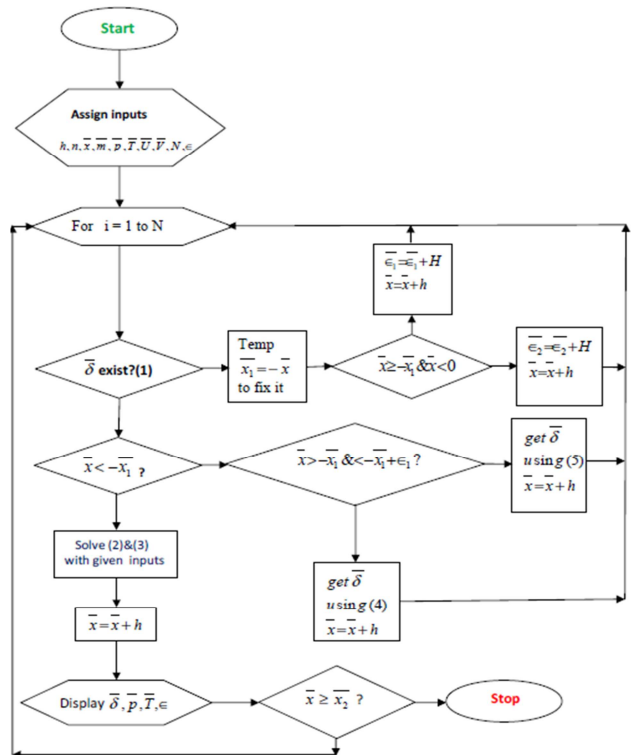
Fig. 1. Lubrication of Asymmetric rollers.

The values of the flow index n is considered to be greater than unity for dilatants fluid, equal to unity Newtonian and less than unity Pseudo plastic. The sliding parameter \bar{U} is chosen to lie between 1.0 and 1.4. The parameter \bar{U} arises due to the consideration of anti-symmetric conditions and is important because the presence of sliding ($\bar{U} > 1$) is likely to produce greater pressure and temperature as compared to that of pure rolling ($\bar{U} = 1$). The significance of \bar{U} along with n has been demonstrated through table and graphs for $\beta \neq 0$. For the numerical calculation, the following representative values have been used: $U_2 = 400 \text{ cm / s}$, $h_0 = 10^{-4} \text{ cm}$, $\alpha = 1.6 \times 10^{-9} \text{ dyne}^{-1} \text{ cm}^2$, $R = 3 \text{ cm}$, $\bar{\gamma} = 5$, $c_1 = 0.6 \times 10^{-9} \text{ pa}^{-1}$, $c_2 = 1.7 \times 10^{-9} \text{ pa}^{-1}$, $D_T = 0.65 \times 10^{-3} \text{ K}^{-1}$.

It may be noted that the flow configuration considered herein includes several known situations as limiting cases: for instance when $U_1 = U_2$, and m is constant, it reduces to the case examined by Sinha and Singh [35]; for the case $\beta = 0$, this is the case considered by Sinha and Raj [36]. Further, when $U_1 = U_2$, and $\beta \neq 0$, the present analysis is equivalent to that of Prasad et al. [15].

3.1 Numerical Solutions

The Reynolds and the energy equations are coupled through \bar{m} , and contain two unknowns $\bar{\delta}$ (the locus of point at which $\frac{\partial u}{\partial y} = 0$) and the initial value of \bar{r} . These unknowns are also present in equation (36). As there is no symmetry ($\bar{U} \neq 1$), it is necessary to solve (36) for $\bar{\delta}$. The actual process followed for numerical computation of $\bar{\epsilon} - \bar{\delta}$ is briefly described below in the flow chart.



3.2 Pressure profile

The qualitative behavior of the pressure profile \bar{p} for different values of n , \bar{V} , and \bar{U} has been numerically calculated by solving Reynolds equation (in conjunction with energy equation) and presented in Figs. 2-4. It can be observed from the Fig. 2 that the lubricant pressure increases with n . This is in conformity with the observations made by [15,37,38] for cylindrical roller bearings. Figure 3 indicates that the pressure profile drawn for different values of squeezing parameter \bar{V} with fixed $\bar{U} = 1.2$ and $n = 1.15$. is similar in nature but look different only up to the point of maximum pressure and then later almost identical/ overlapping because

there is sharp decrease in compressible pressure there near the outlet [39]. This shows that the squeezing and the compressible effects are not very significant near the outlet in case of rolling and sliding condition. Further, the pressure for $\bar{V}=0$ is lower when compared to that of $\bar{V}=0.2$, and higher than in comparison to $\bar{V}=-0.2$.

Pressure profile for $\bar{u}=1.2, \bar{v}=0.1$

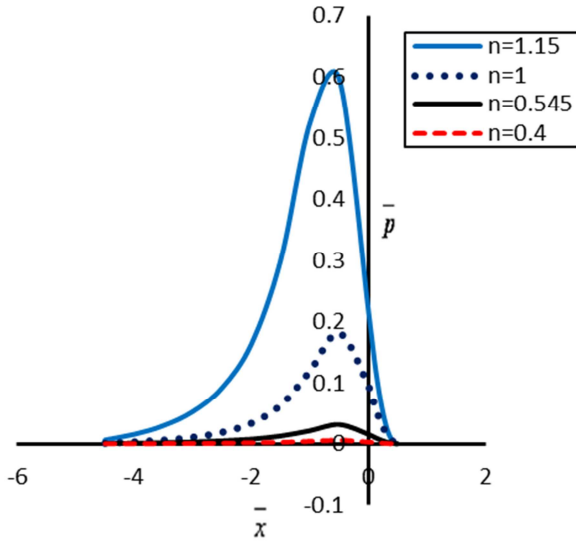


Fig. 2. Pressure profile \bar{p} versus \bar{x} .

Pressure profile for $\bar{u}=1.2, n=1.15$

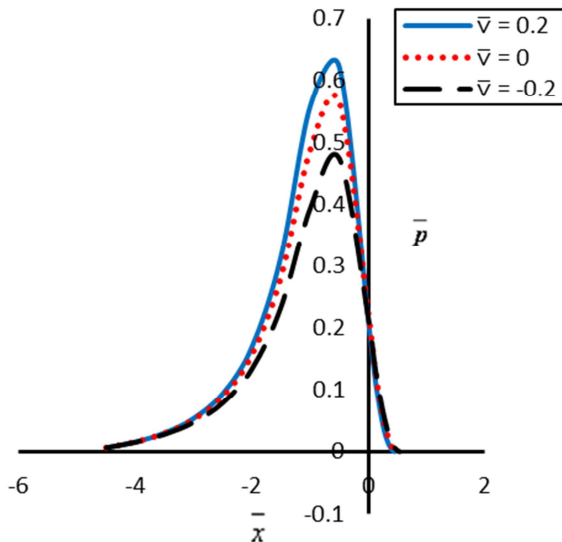


Fig. 3. Pressure profile \bar{p} versus \bar{x} .

This result is almost similar to that of [3] for compressible – squeezing with line contact. However, the above trend does not match with symmetric and incompressible result [6]. Further, one can observe from Fig. 4 that the

pressure curves drawn for $\bar{U}=1, \bar{U}=1.2$, and $\bar{U}=1.4$ are similar in nature. In fact, the pressure increases with \bar{U} only up to the point of maximum pressure; and there after they are identical. The increase of pressure here indicates increase in load [37]. Jang and Khonsari [40] established that hydrodynamic pressure increases with decrease in slide to roll ratio. Further, the maximum pressure increases with n is shown in Fig. 5. This trend seems to be reversed to that of [16,41].

Pressure profile for $n=1.15, \bar{v}=0.2$

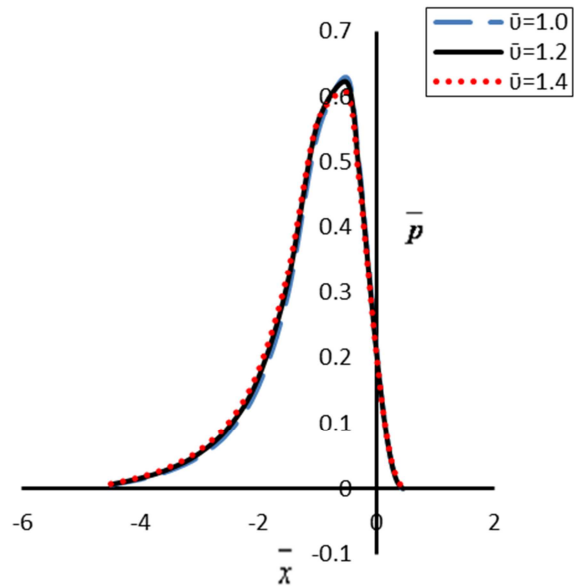


Fig. 4. Pressure profile \bar{p} versus \bar{x} .

Maximum Pressure with 'n'

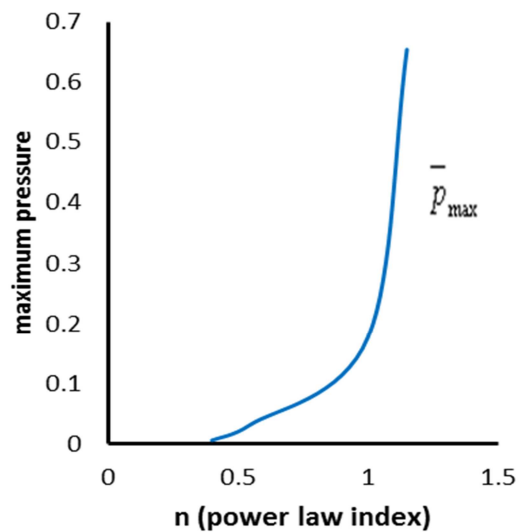


Fig. 5. \bar{p}_{\max} profile with n .

3.3 Temperature profile

The results of the fluid film temperature \bar{T} obtained by solving the differential equations (38) and (39) can be analyzed through Figs. 6-8, for various values of n , \bar{V} , and \bar{U} . Qualitatively the temperature increases with \bar{x} up to the point of maximum pressure and then decreases throughout the outlet region which is quite similar to that of temperature profile shown by [24,42].

Further, Fig. 6 shows that \bar{T} increases with n . This shows that the temperature \bar{T} for dilatant fluid is higher than that of Newtonian and pseudo plastic fluids both. This kind of behavior was also observed by [15,37] for pure rolling and rolling/sliding. It can be observed from Fig. 7 that the temperature \bar{T} increases significantly as \bar{V} decreases for fixed $\bar{U}=1.2$ and $n=1.15$. This \bar{T} trend for compressible fluids is just reversed to that of incompressible fluids [6,43]. Further, the qualitative analysis of \bar{T} for pure rolling and rolling/ sliding conditions of the surfaces has been shown in Fig. 8. From the figure it can be noted that the temperature \bar{T} increases with \bar{U} . Also, it indicates that the sliding temperature is higher than that of pure rolling. The similar results were obtained by [37,44-46].

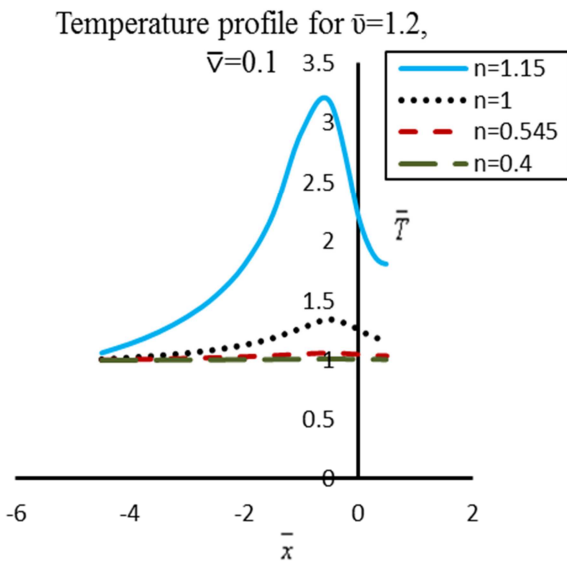


Fig. 6. Temperature profile \bar{T}_m versus \bar{x} .

Temperature profile for $\bar{v}=1.2, n=1.15$

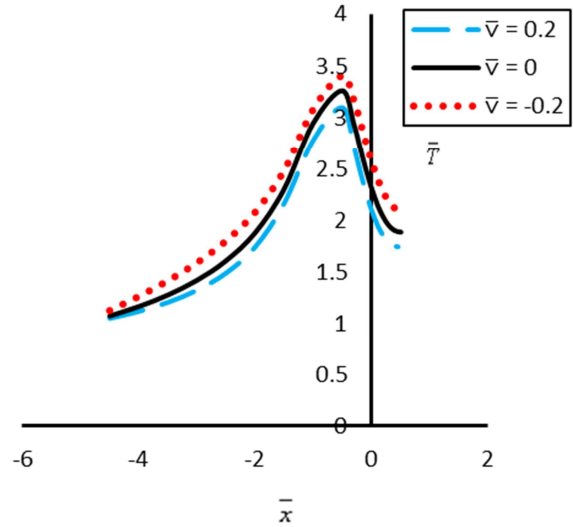


Fig. 7. Temperature profile \bar{T}_m versus \bar{x} .

Temperature profile for $n=1.15, \bar{v}=0.2$

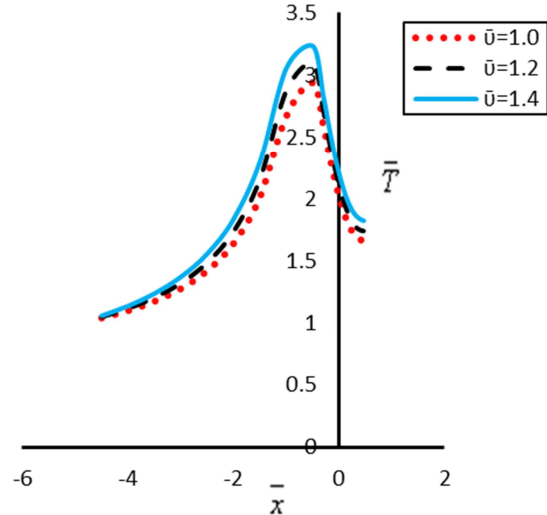


Fig. 8. Temperature profile \bar{T}_m versus \bar{x} .

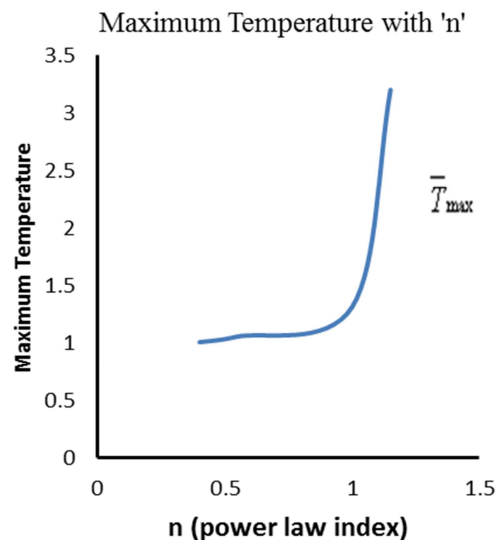


Fig. 9. \bar{T}_{max} profile with n .

The maximum lubricant temperature increases with n is shown in Fig. 9, and is in conformity with the previous findings of [37,39,41].

3.4 ε - $\bar{\delta}$ profile

The qualitative behaviors of $\bar{\delta}$ with actual numerical computations (roughly mentioned in Fig. 1 for various values of the parameters \bar{V} and n are presented in Figs. 10 and 11 respectively.

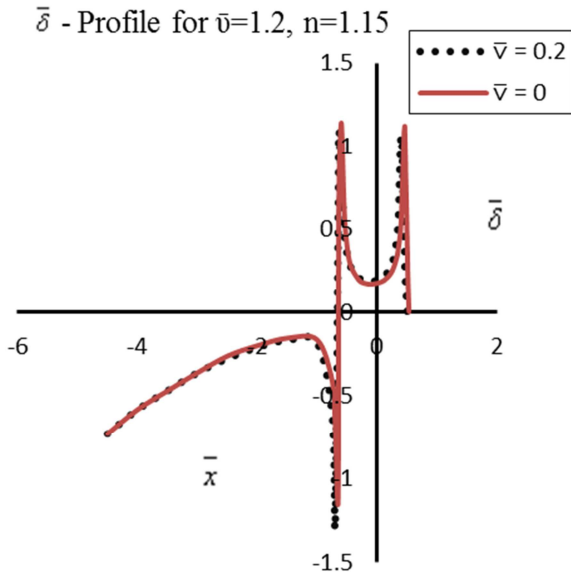


Fig. 10. $\bar{\delta}$ -profile versus \bar{x} .

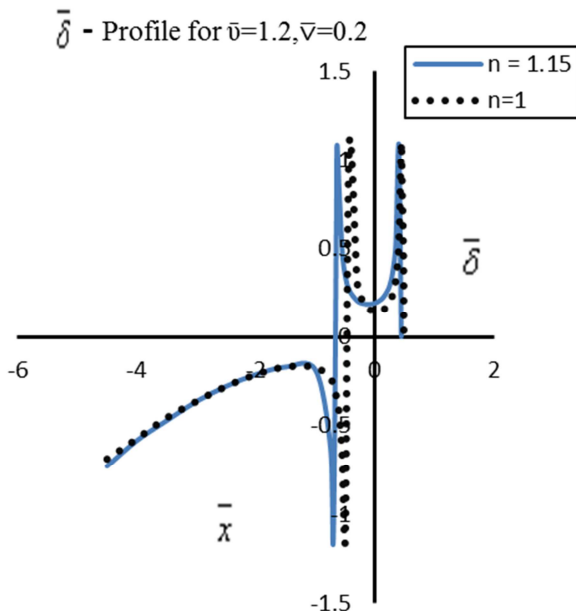


Fig. 11. $\bar{\delta}$ -profile versus \bar{x}

The $\bar{\delta}$ -profile, with and without squeezing, is shown in Fig. 10 and these two profiles are

almost similar/ identical. The next Fig. 11 gives the analysis of $\bar{\delta}$ -profile for dilatants and Newtonian fluids with fixed $\bar{U} = 1.2$ and $\bar{V} = 0.2$. Here $\bar{\delta}$ profile indicates that the points of maximum pressure for Newtonian and dilatants fluids are respectively made nearer and farther from the centre point of contact.

3.5 Consistency Profile

The quality behavior of the consistency \bar{m} which varies with pressure \bar{p} and the temperature \bar{T} (see equation (41)) is presented in Fig. 12 for $\bar{U} = 1.2$, $n = 1.15$ and $\bar{V} = -0.1$.

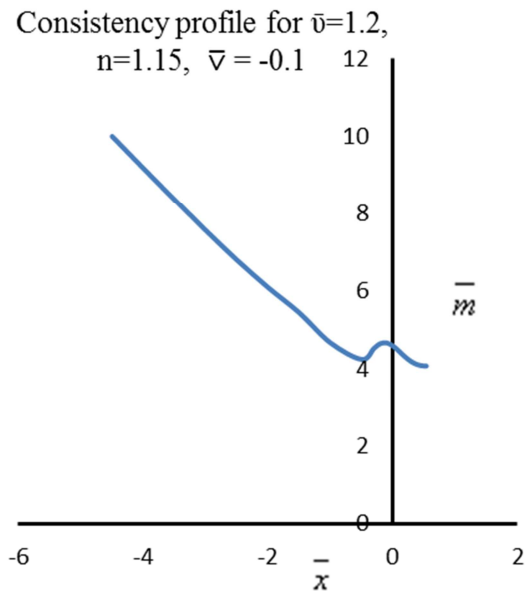


Fig. 12 . Consistency profile \bar{m} versus \bar{x}

It may be observe from this figure that \bar{m} decreases throughout the inlet region up to the pressure peak. Then it increases a little up to $\bar{x} = 0$ and latter decreases again throughout outlet region. In fact, \bar{m} profile seems to be just reverse to that of the temperature in the complete inlet region. In other words it can be said that the consistency decreases when temperature increases. Truly speaking, the decrease / increase in the consistency are the decrease / increase in the resultant of the pressure and the temperature. We may infer that the temperature has significant effect on consistency in comparison to the corresponding pressure. The similar kind of trend was obtained by [43].

3.6 Density profile

The lubricant density $\bar{\rho}$ related with pressure \bar{P} and the temperature \bar{T} (see equation (40)) may be analyzed through the Fig. 13. It may be observed that the density profile follows the similar trend as that of consistency profile.

Therefore, it may be concluded that the temperature has also more significant effect on density in comparison to that of pressure.

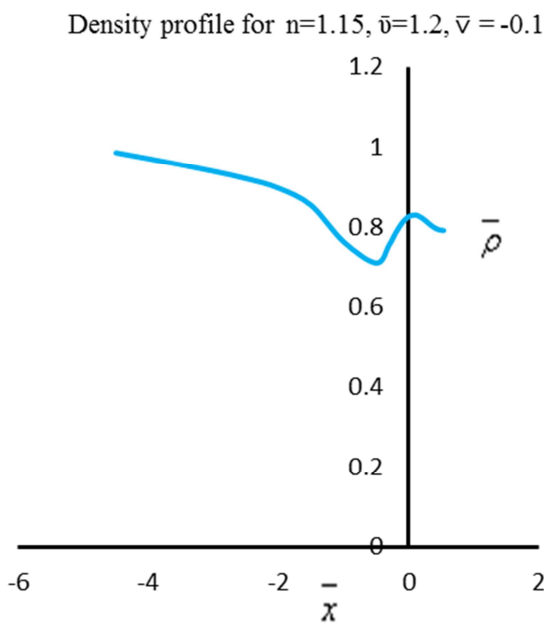


Fig. 13. Density profile $\bar{\rho}$ versus \bar{x} .

3.7 Point of maximum Pressure and Cavitation points

The Reynolds equation (34) in the region ($-x_1 \leq x \leq x_2$) is solved for cavitation points \bar{x}_2 using the conditions $\bar{p}_2 = 0$ and $\frac{d\bar{p}_2}{dx} = 0$ for different values of n , \bar{V} , and are presented in Table 1 with and without squeezing. The cavitation points are shifted towards the center point of contact as \bar{V} increases for any fixed value of n . This trend does not match for symmetric with incompressibility result [6]. However, for fixed \bar{V} , the cavitation points of

non-Newtonian fluids are shifted towards the centre point of contact in comparison to that of Newtonian fluid. Categorically, for a fixed \bar{V} , the cavitation point decreases with n for all $n \leq 1$ but not for $n=1.15$.

The numerical values of \bar{x}_1 , the points of maximum pressure, for different values of n and \bar{V} are presented in Table 1 along with the cavitation points. It may be observed from this table that \bar{x}_1 decreases with \bar{V} , i.e. they are shifted towards the centre point of contact as \bar{V} decreases for each fixed value of n . A similar trend was observed by [6,43]. Further for a fixed value of \bar{V} , \bar{x}_1 increases as n decreases for Newtonian and Pseudo plastic fluids [43]. But, the trend changes for dilatants fluid.

3.8 Load and Traction

The numerical values of the normal load carrying capacity \bar{W} , the traction forces \bar{T}_{F+} at $\bar{y} = \bar{h}$ (upper surface) and \bar{T}_{F-} at $\bar{y} = -\bar{h}$ (lower surface) are computed and presented in the form of Table 2. It can be seen from the table that \bar{W} increases with n for each value of \bar{V} for fixed $\bar{U} = 1.2$ [37, 47]. Further the load decreases as \bar{V} increases in case of Newtonian and pseudo plastic fluids [6,43]. However, the load increases with \bar{V} for dilatants fluids.

The traction forces \bar{T}_{F-} and \bar{T}_{F+} has been evaluated for various values of n with and without squeezing, and follow the same trend as that of load. Further, it is to be noted that the traction forces at the lower surfaces are low as compared to that of the upper surface in case of Newtonian and pseudo plastic fluids for different values of \bar{V} . But, non-Newtonian dilatants fluid follows some mixed trend for different values of \bar{V} .

Table 1. Points of maximum pressure and cavitations.

n/m_0	Squeeze (\bar{V}) \rightarrow	0.2	0.1	0	-0.1	-0.2
1.15/0.56	\bar{r}	-3.217899	-2.713841	-2.213761	-1.719251	-1.231699
	\bar{x}_1	0.664004	0.645405	0.627405	0.606005	0.583005
	\bar{x}_2	0.464288	0.488188	0.512863	0.537587	0.561862
1.0/0.75	\bar{r}	-3.728461	-3.235166	-2.739885	-2.242121	-1.743979
	\bar{x}_1	0.470407	0.454807	0.440407	0.426407	0.413008
	\bar{x}_2	0.505988	0.536862	0.568187	0.599986	0.632186
0.545/86.0	\bar{r}	-3.698291	-3.214899	-2.730269	-2.244369	-1.757370
	\bar{x}_1	0.503006	0.485807	0.469407	0.453007	0.437407
	\bar{x}_2	0.469588	0.498988	0.528862	0.559287	0.590187
0.4/126.0	\bar{r}	-3.689511	-3.208103	-2.725302	-2.241417	-1.756477
	\bar{x}_1	0.516006	0.498706	0.481807	0.465007	0.448807
	\bar{x}_2	0.461863	0.490863	0.519588	0.549187	0.579587

Table 2. Load, Traction Forces, Maximum Pressure and Temperature.

n/m_0	Squeeze (\bar{V}) \rightarrow	0.2	0.1	0	-0.1	-0.2
1.15/0.56	\bar{W}	1.067529	1.028345	0.980613	0.917716	0.836443
	\bar{T}_{F+}	3.658551	3.500792	3.307765	3.07431	2.784633
	\bar{T}_{F-}	3.670508	3.504292	3.30484	3.064961	2.770892
	\bar{p}_{max}	0.654358	0.620095	0.581410	0.534853	0.479133
	\bar{T}_{max}	3.204486	3.259898	3.320452	3.734473	3.428965
1.0/0.75	\bar{W}	0.265008	0.274883	0.274883	0.291903	0.297764
	\bar{T}_{F+}	0.84411	0.866352	0.886035	0.902093	0.911975
	\bar{T}_{F-}	0.839128	0.86094	0.880494	0.896071	0.905897
	\bar{p}_{max}	0.176292	0.183137	0.189353	0.194569	0.198188
	\bar{T}_{max}	1.318532	1.346509	1.377697	1.413827	1.455596
0.545/86.0	\bar{W}	0.049622	0.051109	0.052587	0.054041	0.055429
	\bar{T}_{F+}	0.166225	0.169777	0.172861	0.175865	0.178619
	\bar{T}_{F-}	0.158302	0.169421	0.172454	0.175318	0.178007
	\bar{p}_{max}	0.03075	0.031717	0.032668	0.033594	0.034468
	\bar{T}_{max}	1.057986	1.062688	1.068191	1.074813	1.08309
0.4/126.0	\bar{W}	0.009421	0.009675	0.009934	0.010195	0.010456
	\bar{T}_{F+}	0.032163	0.0327	0.033233	0.03377	0.034296
	\bar{T}_{F-}	0.032235	0.032742	0.033252	0.033762	0.034272
	\bar{p}_{max}	0.005705	0.005867	0.006029	0.006192	0.006354
	\bar{T}_{max}	1.011027	1.011909	1.012952	1.014228	1.01585

4. CONCLUSION

The non-Newtonian power lubrication of asymmetric rollers is studied. The effects of pressure and temperature on the lubricant consistency and density are taken into consideration along with squeezing motion and cavitations. Some important bearing characteristics of compressible fluid are analyzed. The results are compared with and without squeezing. The following conclusions are made:

- (1) The temperature variation within the contact is greatly influenced by the squeeze motion of the compressible lubricants.
- (2) The temperature has significant effect on consistency and density in comparison to the corresponding pressure.
- (3) The load increases with n significantly which justifies the consideration of non-Newtonian lubricant.
- (4) The load decreases as squeezing parameter \bar{V} increases for Newtonian and pseudo plastic fluids. But the trend is just reversed for dilatants fluid. The traction forces follow the same trends as the load.
- (5) The sliding parameter \bar{U} has more significance on temperature (see Fig. 8) and less on pressure (see Fig. 4)
- (6) Pressure \bar{p} increases as \bar{V} increases, however, it is not the same for incompressible with symmetry.
- (7) The cavitation points move towards the central line of contact as \bar{V} increases. But for symmetric with incompressible, it is not true.

Nomenclature

- c_1, c_2 : Density-pressure coefficients
- c_n : $\frac{1}{2} \left(\frac{2n+1}{n} \right)^n \left(\frac{U}{h_0} \right)^n \sqrt{\frac{2R}{h_0}}$
- D_T : Density-temperature coefficient
- h : Lubricant film thickness
- h_0 : Minimum film thickness
- \bar{h} : h / h_0 etc.
- m : Lubricant consistency etc.
- m_0 : Consistency at ambient pressure and temperature

- \bar{m} : $2 m c_n c_1$ etc.
- n : Consistency index of the power law lubricant
- p : Hydrodynamic pressure
- P_1 : Pressure in the region $-\infty < x \leq -x_1$
- P_2 : Pressure in the region $-x_1 < x \leq x_2$
- \bar{p} : $c_1 p$ etc.
- R : Radius of the equivalent cylinder
- T : Lubricant temperature
- T_1 : Film temperature for $y \geq \delta$ in region-I etc.
- T_0 : Ambient temperature
- \bar{T} : βT etc.
- T_{Fh} : Traction force at the upper surface
- \bar{T}_{Fh} : Dimensionless traction force ($= - (2 \alpha T_{Fh} / h_0)$) etc.
- U_1, U_2 : Velocities of the cylinders at $y = -h$ and $y = h$ respectively
- u : Velocity of the lubricant in x-direction
- \bar{u} : $\frac{u}{U_1}$
- V : Squeezing velocity of the surface
- \bar{V} : $\frac{V}{U_1} \sqrt{\frac{2R}{h_0}}$
- v : Velocity of the lubricant in y-direction
- W : Load in y-direction
- \bar{W} : Dimensionless load ($= \alpha W / (Rh_0)^{1/2}$)
- x, y : Co-ordinate axes
- \bar{x} : Dimensionless distance in x-direction ($= x / (2Rh_0)^{1/2}$) etc.
- x_1 : Point of maximum pressure
- x_2 : Cavitation point
- α : Pressure coefficient
- β : Temperature coefficient
- δ : Location of points where velocity gradient $\frac{\partial u}{\partial y} = 0$
- $\bar{\delta}$: $\frac{\delta}{h_0}$
- $\bar{\gamma}$: $\left(\frac{\beta}{\rho_0 c_1 c_p} \right)$

REFERENCES

- [1] J. Manojlović: *Dynamics of SAMs in Boundary Lubrication*, Tribology in Industry, Vol. 35, No. 3, pp. 200-207, 2013.
- [2] R. Usha, Rukmani Sridharan: *An investigation of a squeeze film between two plane annuli*, Journal of Tribology, Vol. 120, No. 3, pp. 610-615, 1988.
- [3] M.J. Jaffar: *Squeeze films between a rigid cylinder and an elastic layer bonded to a rigid foundation*, Tribology International, Vol. 40, No. 3, pp. 567-572, 2007.
- [4] D. Dowson, P.H. Markho, D.A. Jones: *The lubrication of lightly loaded cylinders in combined rolling, sliding and normal motion, part-i, theory*, ASME Journal of Lubrication Technology, Vol. 98, No. 4, pp. 509-517, 1976.
- [5] P. Sinha, J.B. Shukla, K.R. Prasad, C. Singh: *Non-Newtonian power-law fluid lubrication of lightly loaded cylinders with normal and rolling motion*, Wear, Vol. 89, No. 3, pp. 313-322, 1983.
- [6] D. Prasad, P. Singh, P. Sinha: *Thermal and squeezing effects in non-newtonian fluid film lubrication of rollers*, Wear, Vol. 119, No. 2, pp. 175-190, 1987.
- [7] L. Rong-Tsong, B.J. Hamrock: *Squeezing and entraining motion in non-conformal line contacts: part-I, Hydrodynamic lubrication*, ASME, Journal of Tribology, Vol. 111, No. 1, pp. 1-7, 1989.
- [8] J-R Lin, R-F Lu, T-B Chang: *Derivation of Dynamic Couple-Stress Reynolds Equation of Sliding Squeezing Surfaces and Numerical Solution of Plane Inclined Slider Bearings*, Tribology International, Vol. 36, No. 9, pp. 679-685, 2003.
- [9] N.M. Bujurke, N.B. Naduvinamani, D.P. Basti: *Effect of surface roughness on the squeeze film lubrication between curved annular plates*, Industrial Lubrication and Tribology, Vol. 59, No. 4, pp. 178-185, 2007.
- [10] N.B. Naduvinamani, Syeda Thasneem Fathima, Salma Jamal: *Effect of roughness on hydrodynamic squeeze films between porous rectangular plates*, Tribology International, Vol. 43, pp. 2145-2151, 2010.
- [11] Li-Ming Chu, Jin Yuan Lai, Chi-Hui Chien, Wang Long Li: *Effect of surface forces on pure squeeze thin film EHL motion of circular contacts*, Tribology International, Vol. 43, No. 3, pp. 523-531, 2010.
- [12] Jaw-Ren Lin: *Non-Newtonian squeeze film characteristics between parallel annular disks: rabinowitsch fluid model*, Tribology International, Vol. 52, pp. 190-194, 2012.
- [13] S. Kondo, R.S. Sayles, M.J.S. Lowe: *A combined optical-ultrasonic method of establishing the compressibility of high-pressure oil and grease films entrapped in a ball on flat contact*, Journal of Tribology, Vol. 128, No. 1, pp. 155-167, 2006.
- [14] Jonas Stahl, O. Jacobson: *Compressibility of lubricants at high pressure*, Tribology Transactions, Vol. 46, No. 4, pp. 592-599, 2003.
- [15] D. Prasad, P. Singh, P. Sinha: *Non-uniform temperature in non-Newtonian compressible fluid film lubrication of rollers*, ASME Journal of Tribology, Vol. 110, No. 4, pp. 653-658, 1988.
- [16] Hsiao-Ming Chu, Wang-Long Li, Yuh-Ping Chang: *Thin film elastohydrodynamic lubrication – A power law fluid model*, Tribology International, Vol. 39, No. 11, pp. 1474-1481, 2006.
- [17] L. Moraru, T.G. Keith: *Lobatto point quadrature for thermal lubrication problems involving compressible lubricants. EHL applications*, Journal of Tribology, Vol. 129, No. 1, pp. 194-198, 2007.
- [18] Mircea D. Pascovici, Traian Cicone, Victor Marin: *Squeeze process under impact in highly compressible porous layers, imbibed with liquids*, Tribology International, Vol. 42, No. 10, pp. 1433-1438, 2009.
- [19] T.A. Stolarski: *Numerical modeling and experimental verification of compressible squeeze film pressure*, Tribology International, Vol. 43, No. 1-2, pp. 356-360, 2010.
- [20] G. Bayada, L. Chupin: *Compressible fluid model for hydrodynamic lubrication cavitation*, Journal of Tribology, Vol. 135, No. 4, pp. 041702-1 to 041702-13, 2013.
- [21] W. Habchi, S. Bair: *Quantitative compressibility effects in thermal elastohydrodynamic circular contacts*, Journal of Tribology, Vol. 135, No. 1, pp. 011502-1 to 011502-10, 2013.
- [22] Nadim A. Diab, Issam Lakkis: *Modeling squeeze films in the vicinity of high inertia oscillating microstructures*, Journal of Tribology, Vol. 136, No. 2, pp. 021705-1 to 021705-8, 2014.
- [23] Andreas Almqvist, John Fabricius, Roland Larsson, Peter Wall: *A new approach for studying cavitation in lubrication*, Journal of Tribology, Vol. 136, No. 1, pp. 011706-1 to 011706-7, 2014.
- [24] Li-Ming Chu, Hsiang-Chen Hsu, Jaw-Ren Lin, Yuh-Ping Chang: *Inverse approach for calculating temperature in EHL of line contacts*, Tribology International, Vol. 42, No. 8, pp. 1154-1162, 2009.

- [25] P.C. Mishra: *Analysis of a Rough Elliptic Bore Journal Bearing using Expectancy Model of Roughness Characterization*, Tribology in Industry, Vol. 36, No. 2, pp. 211-219, 2014.
- [26] Yuchuan Liu, Jane Wang, Ivan Krupka, Martin Hartl, Scott Bair: *The shear thinning elastohydrodynamic film thickness of a two component mixture*, Journal of Tribology, Vol. 130, No. 2, pp. 021502-1 to 021502-7, 2008.
- [27] R.I. Tanner: *Engineering Rheology*, Oxford University Press, 2nd Edn, PP. 129-133, Oxford, 2000.
- [28] Fredrik Sahlin, Sergie B. Glavatskin, Torbjorn Almqvist, Roland Larson: *Two dimensional CFD analysis of micro-patterned surfaces in hydrodynamic lubrication*, Journal of Tribology, Vol. 127, No. 1, pp. 96-102, 2005.
- [29] A.A. Minewitsch: *Some Developments in Triboanalysis of Coated Machine Components*, Tribology in Industry, Vol. 33, No. 4, pp. 153-158, 2011.
- [30] H.S. Cheng, B. Sternlicht: *A numerical solution for pressure, temperature and film thickness between two infinitely long lubricate rolling and sliding cylinders, under heavy loads*, Journal of Basic Engineering, Vol. 87, pp. 695, 1965.
- [31] P. Yang, J. Wang, M. Kaneta: *Thermal and non-Newtonian numerical analyses for starved EHL line contacts*, Journal of Tribology, Vol. 128, No. 2, pp. 282-290, 2006.
- [32] J.B. Shukla, M. Isa: *Thermal effects in squeeze films and externally pressurized bearing with power-law lubricants*, Wear, Vol. 51, No. 2, pp. 237-251, 1978.
- [33] O. Pinkus, B. Sternlicht: *Theory of hydrodynamic lubrication*, Mc Graw Hill Publication, New York, pp. 286, 1961.
- [34] Hashimoto and M. Mongkolwongrojn, C. Prabkaew: *Non-Newtonian turbulent lubrication theory based on friction law of fluid*, Transactions of Japan Society of Mechanical Engineers, Part C, Vol. 60, pp. 1006-1012, 1994.
- [35] P. Sinha, C. Singh: *Lubrication of cylinder on a plane with a non-newtonian fluid considering cavitation*, ASME Journal Of Lubrication Technology, Vol. 104, No. 2, pp. 168-172, 1982.
- [36] P. Sinha, S.A. Raj: *Exponential viscosity variation in the non-newtonian lubrication of rollers considering cavitations*, Wear, Vol. 87, No. 1, pp. 29-38, 1983.
- [37] D. Prasad, J.B. Shukla, P. Singh, P. Sinha, R.P. Chhabra: *Thermal effects in lubrication of asymmetrical rollers*, Tribology International, Vol. 24, No. 4, pp. 239-246, 1991.
- [38] S.H. Wang, D.Y. Hua, H.H. Zang: *A full numerical EHL solution for line contacts under pure rolling condition with a non-Newtonian rheological model*, ASME, Journal of Tribology, Vol. 110, No. 4, pp. 583-586, 1988.
- [39] P.K. Saini, P. Kumar, P. Tandon: *Thermal elastohydrodynamic lubrication characteristics of couple stress fluids in rolling/sliding line contacts*, Journal of Engineering Tribology, Vol. 221, No. 2, pp. 141-153, 2007.
- [40] J.Y. Jang, M.M. Khonsari: *Elastohydrodynamic line contact of compressible shear thinning fluids with consideration of the surface roughness*, ASME, Journal of Tribology, Vol. 132, No. 3, pp. 034501-1 to 034501-6, 2010.
- [41] Punit Kumar, S.C. Jain, S. Ray: *Thermal EHL lubrication of rolling/sliding line contacts using a mixture of Newtonian and power law fluids*, 2008, Journal of Engineering Tribology, Vol. 222, No. 1, pp. 35-49, 2008.
- [42] A. Almqvist, J. Dasht: *The homogenization process of the Reynolds equation describing compressible liquid flow*, Tribology International, Vol. 39, No. 9, pp. 994-1002, 2006.
- [43] D. Prasad, P. Singh, Prawal Sinha: *Thermal and inertia effects in hydrodynamic lubrication of rollers by a power law fluid considering cavitations*, Journal of Tribology, Vol. 115, No. 2, pp. 319-326, 1993.
- [44] M.K. Ghosh, B.J. Hamrock: *Thermal EHD lubrication of line contacts*, ASLE, Vol. 28, pp. 159-171, 1985.
- [45] F. Sadeghi, T.A. Dow, R.R. Johnson: *Thermal effects in rolling/sliding contacts: part-3, Approximate method for prediction of mid-film temperature and sliding traction*, Journal of Tribology, Vol. 109, No. 3, pp. 519-523, 1987.
- [46] P.N. Bogdanovich, D.V. Tkachuk: *Temperature distribution over contact area and 'Hot Spots' in rubbing solid contact*, Tribology International, Vol. 39, No. 11, pp. 1355-1360, 2006.
- [47] D. Prasad, P. Singh, Prawal Sinha: *Thermal and inertia effects in rollers with power law lubricant having temperature and pressure dependent consistency*, Indian Journal of Pure and Applied Mathematics, Vol. 24, No. 4, pp. 305-320, 1992.